www.czasopisma.pan.pl PAN www.journals.pan.pl
Opto-Electronics Review 27 (2019) 70–78

Contents lists available at ScienceDirect

Opto-Electronics Review

journal homepage: http://www.journals.elsevier.com/opto-electronics review

Junction configurations and their impacts on Cu(In,Ga)Se_2 based solar cells performances

N. Guirdjebaye [a,*], S. Ouédraogo [b], A. Teyou Ngoupo [a], G.L. Mbopda Tcheum [a], J.M.B. Ndjaka [a]

[a] Département de Physique, Faculté des Sciences, Université de Yaoundé 1, BP 812, Yaoundé, Cameroon
[b] Laboratoire des Matériaux et Environnement (LAME), UFR-SEA, Université de Ouagadougou, BP 7021, Ouaga 03, Burkina Faso

ARTICLE INFO

Article history:
Received 8 October 2018
Received in revised form 18 January 2019
Accepted 6 February 2019
Available online 19 March 2019

Keywords:
Defect density
P+ layer
Back surface field
CIGS
SCAPS-1D

ABSTRACT

One dimension solar cells simulator package (SCAPS) is used to study the possibility of carrying out thin CIGS solar cells with high and stable efficiency. In the first step, we modified the conventional ZnO:B/i-ZnO/CdS/SDL/CIGS/Mo structure by substituting the SDL layer with the P+layer, having a wide bandgap from 1 to l.12 eV. Then, we simulated the J-V characteristics of this new structure and showed how the electrical parameters are affected. Conversion efficiency of 18.46% is founded by using 1.1 μm of P+layer thickness. Secondly, we analyze the effect of increase thickness and doping density of CIGS, CdS and P+layers on the electric parameters of this new structure. We show that only the short-circuit current density (J_{SC}) and efficiency are improved, reaching respectively 34.68 mA/cm^2 and 18.85%, with increasing of the acceptors density. Finally, we introduced 10 nm of various electron reflectors at the CIGS/Mo interface in the new structure to reduce the recombination of minority carriers at the back contact. High conversion efficiency of 23.34% and better stability are obtained when wide band-gap BSF is used.

1. Introduction

In the last few years, the solar cells constituted by CIGS have impressed many researchers for their increasing efficiency studied in numerous solar industries in the word. This boom has attained the efficiency record of 20.03% in 2013 [1]. In 2016, they reached efficiency of 22.6 [2] and it does not cease increasing because of the improvement of treatment techniques. The CIGS absorber layer has a direct bandgap and a high absorption coefficient (10^5 cm^{-1}) [3], and only few micrometers are required to absorb the maximum photons. Another very important advantage of CIGS absorber layer is its bandgap, which depends to the gallium proportion in this layer. The partial substitution of indium by gallium enlarges the bandgap from 1.02 to 1.69 eV according to the Eq. (1).

$$Eg(x) = 1.02 + 0.67x + bx(x-1). \quad (1)$$

Where x is the proportion of gallium in alloy, i.e. Ga/(Ga + In) ; and b is an optical parameter generally taken between 0.11 and 0.24 [4].

The record efficiency of CIGS thin films solar cells are closely related to the quality of the p-n junction formed between absorber (CIGS) and buffer layer (CdS). Speculations and contradictions were made on the configuration of the CIGS/CdS interface. By using electron microscopy, combined to the catholuminescente spectroscopy, Remero *et al.* [5] proved the experimental existence of a surface layer with electronic properties different from the bulk absorber (CIGS). This wide bandgap surface layer at the CIGS/CdS interface, would be essential to obtain a high efficiency. Indeed, a three-stage co-evaporation process is usually used to produce high efficiency CIGS solar cells. In this process, a Cu-poor composition is intentionally creates on the surface of the CIGS. However, grazing incidence X-ray diffraction, X-ray photoelectron spectroscopy, transmission electron microscopy and energy-dispersive X-ray spectroscopy study did not confirm the existence of this surface layer [6,7]. On the other hand, several publications have shown a diffusion and intermixing of the cadmium atoms (Cd) into the absorber layer or into its surface region during the chemical bath deposition of the CdS layer. An analysis of the chemical composition of the $CuInSe_2$/CdS interface, carried out by Liao *et al.* [8], showed a diffusion of Cd atoms in the first atomic layers of $CuInSe_2$. This diffusion is accompanied by Cu depletion on the absorber surface, thus suggesting that the Cd atoms which act as a donor type defect state occupy Cu sites causing inversion of the surface region of the absorber and a p-n junction within the absorber layer. However, the presence of the surface layer does not appear due to the Cd diffusion. Since, it has been detected in devices without CdS and

* Corresponding author.
E-mail address: innocentguirdjebaye@gmail.com (N. Guirdjebaye).

https://doi.org/10.1016/j.opelre.2019.02.001
1230-3402/

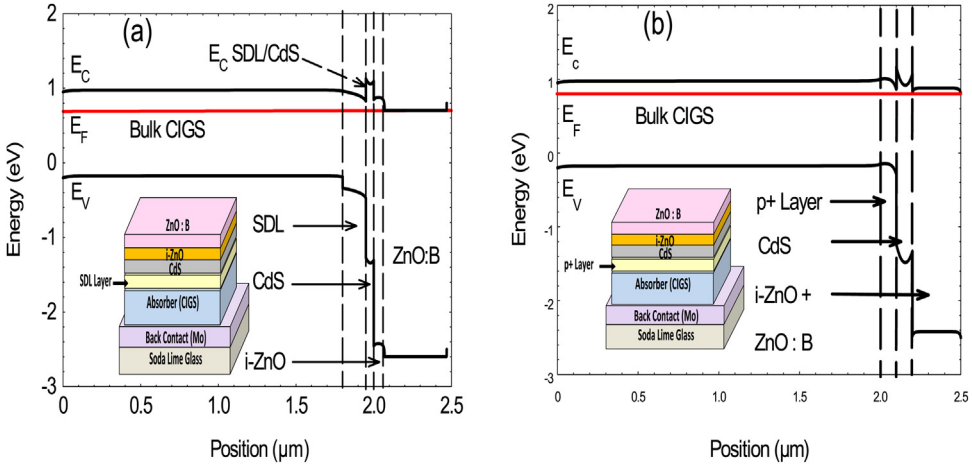

Fig. 1. Schematic representation and band diagram of two cells' configuration at the equilibrium: (a) with SDL layer (conventional structure), (b) with P+ layer (new structure).

might be caused by an n-type surface defect layer (SDL) present at the surface of the CIGS layer [9,10].

Through several influences' profiles, Huang *et al.* [11] show that the influence of the concentration of the donors could be the cause of the pinned of the absorber Fermi level, which affects the buffer/absorber interface and consequently, improves at the same time V_{OC} and J_{SC}.

Another group of researchers propose the presence of P+ layer at the CdS/CIGS interface. Indeed, several publications accompanied by theoretical studies suggest the presence of P+ layer with a high acceptor defect concentration at the CdS/CIGS interface, which creates a strong distortion of the J–V characteristics [12]. This layer plays a destructive role in the efficiency of the solar cell, by increasing recombination at the CdS/CIGS interface.

In first step of this work, we made a compared study of the conventional CIGS solar cell structure (ZnO:B/i-ZnO/CdS/SDL/CIGS/Mo), with a new structure containing P + layer (ZnO:B/i-ZnO/CdS/P+/CIGS/Mo).

In the second step, we proposed to optimize the new structure by focusing on the materials forming the p-n junction (CdS, P+, CIGS). Thus, we have elucidated the influence of thickness, density of donors and acceptors of CIGS, CdS and P + layers on the performance of the cell. The result shows that increasing acceptors density in CIGS and P + layers reduce the photocurrent due to the recombination process in the CIGS absorber. To enhance the performance of new structure, an electron reflector (BSF) is placed at the Mo/CIGS interface and the modifications of the electrical due to this layer are explained.

2. Materials and methods

Two types of configuration are discussed in this work: the conventional structure constituted by SDL layer (ZnO:B/i-ZnO/CdS/SDL/CIGS/Mo/substrate) and the new structure, where the SDL layer is replaced by the P + layer (ZnO:B/i-ZnO/CdS/P+/CIGS/Mo/substrate). The schematic representation and the equivalent band diagram of these configurations, calculated at the thermodynamic equilibrium condition, are given in Fig. 1. The fundamental parts of the cell are the CIGS absorber, CdS buffer layer and the P+ or SDL layer at the CdS/CIGS interface. In the conventional cell structure [Fig. 1(a)] [13], a thin Surface Defect layer (SDL) is founded at the CdS/CIGS interface. This layer is replaced by P+ layer, increase the recombination phenomena at the CdS/CIGS interface deteriorates the electrical parameters of the cell [14]. This result is in agreement with that of works Gloeckler *et al.* [15], which showed that the P + layer used at the CdS/CIGS interface creates recombinations resulting from the states of the junction between the buffer layer and the CIGS absorber. An intrinsic layer ZnO (i-ZnO) is deposited on the top of the buffer layer. This layer is commonly called conducting transparent oxide (CTO) because of its large bandgap, which makes it transparent for most of the solar spectrum. Hagiwara showed that ZnO: Al presents absorption losses, causing a reduction in the quantum efficiency in the areas close to the infrared. Boron-doped ZnO would be more beneficial for the solar cell in term of transparency [16]. The surface of a CTO layer is covered with an anti-reflecting layer MgF_2. This layer decreases the photon reflection and consequently, the number of photon arriving in the absorber layer increases. Table 1 summarizes the parameters used for our reference CIGS solar cell [Fig. 1(b)] in this numerical simulation.

Experimentally, it is extremely difficult to predict the behaviour of the solar cell when some parameters are modified because of its complexity. The numerical simulation is thus an important tool for better understanding the parameters influencing the solar cell. Its advantage is that it allows to foresee new methods of design of a solar cell, while reducing the costs (time, money). In this simulation, AM 1.5 solar radiation is used as a source of lighting with a 1000 W/m^2 power. The reflection on the front and back contacts are fixed to 0.1 and 1, respectively. The other parameters of the simulation are listed in Table 1. Several softwares were elaborated with an aim of simulating thin film solar cells [17]; among those, SCAPS-1D, AMPS can be used. Degrave *et al.* [18] have generally used SCAPS-1D in the simulation of CdTe and CIGS based solar cells. The good agreements between the simulation results and those of the experiment [19,20] motivate us to use this code in our work.

3. Results and dicussion

3.1. Comparison of the performances of the solar cells

If it is clear that modelling is an essential tool to understand and improve solar cells, the interpretation of the results of modelling requires one extreme precaution. We compared the J–V characteristics (Fig. 2) of the two previous structures. It comes out that the efficiency of the conventional cell is improved, compared to the new structure. Indeed, this gain is due to the presence of the SDL layer which reduces the effects of the interface states between absorber and buffer layer. In our previous paper, we have shown that the SDL layer at the CdS/CIGS interface allows to improve the open-circuit voltage and consequently the conversion efficiency by shifting the electrical junction away from the high-recombination hetero-interface between CdS and the SDL [13]. We note that there

Table 1
Parameters used in the numerical simulations for both configurations.

Parameter	Layer				
	CIGS	P+/SDL	CdS	i-ZnO	ZnO:B
W[μm]	Variable	Variable/variable	Variable	0.070	400
E_g[eV]	1.15	1.15/1.3	2.4	3.3	3.3
$\varepsilon/\varepsilon_0$	13.6	13.6/13.6	10	9	9
N_C [cm^{-3}]	2.2×10^{18}	$2.2\times10^{18}/2.2\times10^{18}$x	2.2×10^{18}	2.2×10^{18}	2.2×10^{18}
Nv,[cm^{-3}]	1.8×10^{19}	$1.8\times10^{19}/1.5\times10^{18}$	1.8×10^{19}	1.8×10^{19}	1.8×10^{19}
$V_{th,e}$ [cm/s]	10^7	$10^7/3.9\times10^7$	10^7	10^7	10^7
$V_{th,p}$ [cm/s]	10^7	$10^7/1.4\times10^7$	10^7	10^7	10^7
μ_e [cm^2/Vs]	100	100/10	100	100	100
μ_p [cm^2/Vs]	25	25/1.25	25	25	25
Doping [cm^{-3}]	Variable	Variable/variable	Variable	10^{17}	10^{20}
Bulk defect properties					
Defect density and type: N(cm^{-3})	10^{14}(D)	Variable(D/A)	5×10^{16}(A)	10^{16}(A)	10^{16}(A)
Capture cross-section electrons: σ_e (cm^2)	10^{-15}	10^{-13}	10^{-15}	10^{-15}	10^{-15}
Capture cross-section holes: σ_h (cm^2)	10^{-11}	10^{-15}	5×10^{-13}	5×10^{-13}	5×10^{-13}
Interface properties					
Interface state	CIGS/P+		P+/CdS		
Interface conduction band offset: ΔE_c(eV)	0.3		Variable		
Defect density and type: N(cm^{-3})N[cm^2]	10^{-11}(Neutral)		3×10^{-13} (Neutral)		

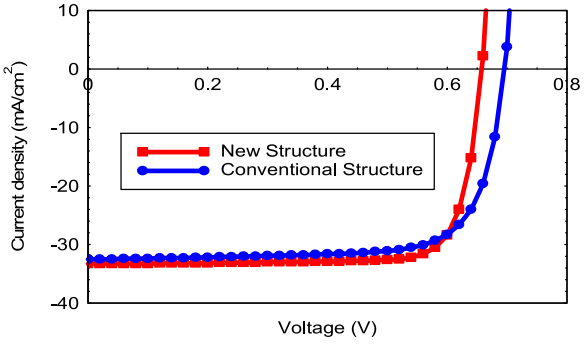

Fig. 2. Comparison of the J–V characteristics of the conventional and new structures.

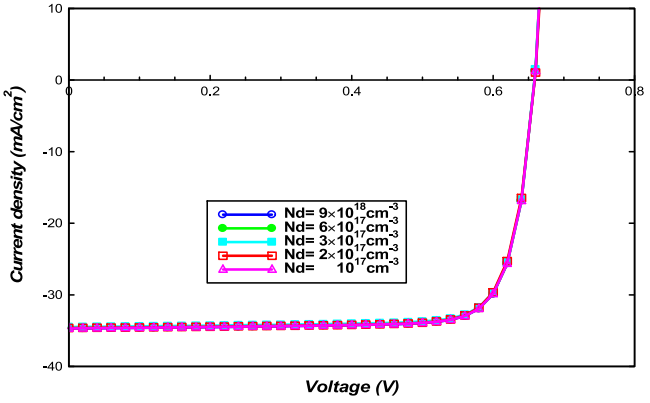

Fig. 3. Influence of the CdS donors' concentration on the J–V characteristics.

Table 2
Comparison of the electrical parameters of the two solar cells.

Solar cell	V_{OC} (V)	J_{SC} (mA/cm^2)	*FF* (%)	η (%)
New structure	0.6579	33.342	80.99	18.46
Conventional structure	0.6959	32.529	75.26	17.70

is a less significant loss of the short-circuit current density (J_{SC}). The band-gap energy of the SDL is higher than of the CIGS bulk regions. This leads to a lower absorption coefficient and a lack of absorption in the long-wavelength portion of the solar spectrum, which affect J_{SC}. When the SDL layer is replaced by the acceptor-like states (P+) layer, the fill-factor and the open-circuit voltage slightly increase. However, when the acceptor density in the P+ layer is high, J–V characteristics undergoes a strong distortion leading to a strong reduction of the fill factor. In this part, the densities of the donors and acceptors in the SDL and P+ layers are similar to have an objective comparison. These results are in good agreement with those reported by Ouédraogo *etal.* [20].

The electrical parameters extracted from J–V characteristics for both configurations are listed in Table 2.

The following sections will be focused on the reference cell by studying the CdS/CIGS junction parameters on the solar cell performances.

3.2. *Effect of CdS donors on the J–V characteristics*

In this part, we analyze the influence of the CdS buffer layer donor density on performances of the new structure. No variation of the J–V characteristics is observed when the donor density is increased (Fig. 3) for a fixed buffer layer thickness. This is simply explained by the fact that this layer does not participate in the production of the photocurrent. The absorption of photons in this layer contributes to reduce the number of photon that reaches in the absorber layer, to contribute to the photovoltaic effect.

3.3. *Donor defect concentration effect on the J–V parameters as function of the CdS thickness*

CdS buffer layer's thickness can contribute to the degradation of the solar cell performances; hence, it is essential to reduce this one in order to limit the absorption losses of photons, which most reached the absorber layer. Thickness variation of this layer, according to its donor's density, also affects electrical parameters of the solar cell (Fig. 4).

The electrical parameters of V_{OC} (Fig. 4c), J_{SC}, [Fig. 4(b)] and the efficiency [Fig. 4(d)] drop with the increase of thickness and donor density of the CdS layer. J_{SC} decreases because the photon absorptions in this layer does not participate in the photovoltaic conversion. On the other hand, *FF* slightly increases under this condition, but reached a limiting value for a thickness higher than 0.01 μm. In addition, the rapid decay of V_{OC}, J_{SC} and the efficiency is simply due to the absorption of the photons in the thick CdS layer; this result is agreement with the result obtained by Topic *et al.* [21].

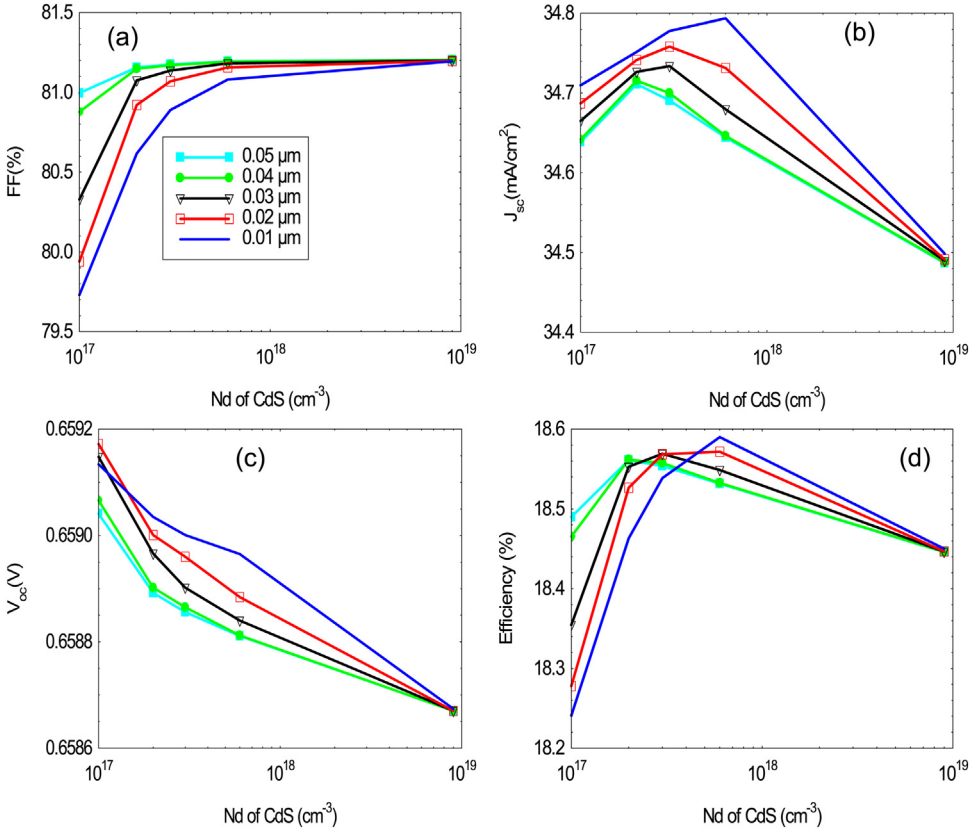

Fig. 4. Influence of CdS layer donor density on the electrical parameters according to the CdS thickness: (a) FF, (b) J_{SC}, (c) V_{OC} and (d) efficiency.

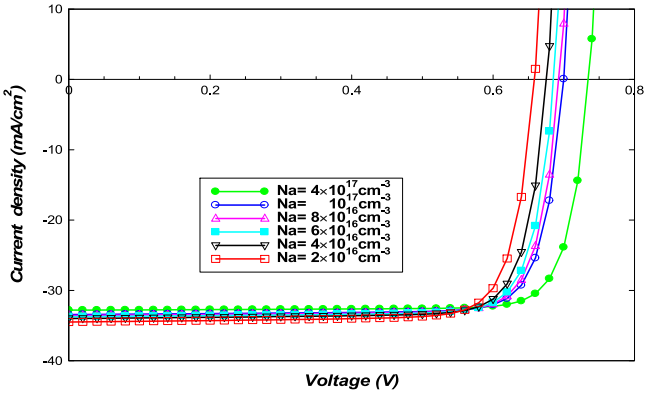

Fig. 5. Current-voltage characteristics according to the CIGS acceptors concentration.

3.4. Acceptors concentration effect of the absorber layer

At the time of the absorber growth much impurities are likely to appear within this one. The most obvious case is the presence of sodium in the absorber, coming from the soda glass. A control of the doping agents is recommended to optimize the performance of the device since to great quantity; they could have an effect on the lifetime of these carriers [22]. Thus, we propose to elucidate the influence of doping on J–V characteristics (Fig. 5). The increase of CIGS layer acceptors' concentration affects the electrical parameters (V_{OC},J_{SC} and η) of the solar cell. The results show that the increase of the acceptor concentration in absorber decreases the recombination velocity, which increases the open circuit voltage. This result is in good agreement with Demtsu *et al.* [23]. The acceptor concentration slightly affects the short-circuit current density when this parameter increases, due to the most recombination process.

3.5. Absorber thickness effect on the electrical parameters

Figure 6 shows the effect of the donors N_d according to the absorber thickness. This study shows that, the electrical parameters (V_{OC}, J_{SC}, FF and η) of the cell practically follow the same trend. The increase of these electrical parameters with the absorber thickness is due to a widening of the space charge region, which extends in the least doped layer, where photovoltaic conversion takes place. On the other hand, the quantity of absorbed photons and the generated electron-hole pair, which contributed to the photocurrent, increase with the absorber layer thickness; this result is in a good agreement with the work of Huang *et al.* [11]. The increasing of the CdS donors' concentration slightly decreases J_{SC}, V_{OC} and η [Fig. 6b)–Fig. 6d)] due to recombination and absorption process in this buffer layer. The increase of FF [Fig. 6a)] is linked to the over-doping of the buffer layer, which makes it possible to obtain a low ohmic contact resistance at the absorber-buffer layer contact.

The best efficiency of the cell is obtained when N_d of CdS layer is between 6×10^{17} and 9×10^{18} cm^{-3}; above these values, variation of the efficiency of the solar cell is almost insignificant whatever the variation of CIGS layer thickness [Fig. 6d)]. This result is in agreement with the experiment result of Igalson *et al.* [24].

Figures 7(a)–(d) show the effect of the absorber thickness on the electrical parameters, for different absorber acceptors density. With SCAPS-1D, this study is made by keeping constant the other parameters of the solar cell. All the electrical parameters have different behaviours when thickness and acceptors' concentration of the absorber increase. The efficiency of the cells increases significantly with the increase of the absorber doping. This increase reaches a maximum limit for a density of about 8×10^{16} cm^{-3}.

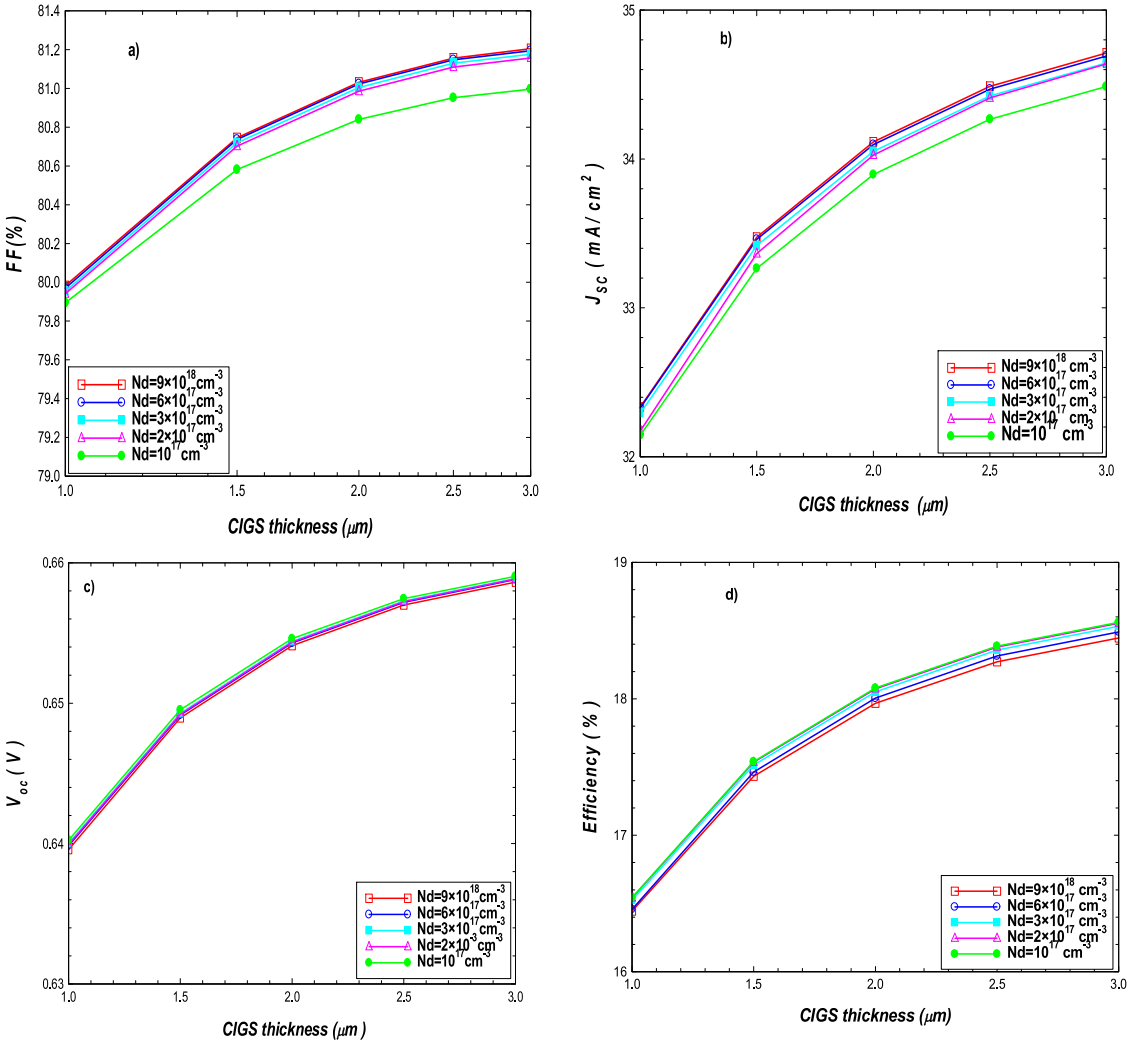

Fig. 6. Evolution of the electrical parameters (V_{OC}, J_{SC} FF and η) as a function of the absorber layer thickness and the CdS donor density.

Beyond this value, there is a reduction in the efficiency independently of CIGS absorber thickness [Fig. 7(d)]. This increase is related to the reduction of the width of the space charge region (W_{SCR}). J_{SC} [Fig. 7(b)]), FF [Fig. 7(a)] and V_{OC} [Fig. 7(c)] also increase with the increase of absorber thickness for a fixed acceptor density.

The increase of V_{OC} with the thickness and the acceptors density of CIGS absorber layer is related to most generation of electron-hole pairs, and, thus the increase of the photocurrent. J_{SC} decreases with the reduction of absorber thickness because of the increase in the recombination rate at the back contact when CIGS layer is very thin. The abrupt decrease of J_{SC} is also explained by the fact that, the absorber being completely depleted, the separation of the Fermi quasi-levels is limited [14]. J_{SC} also decreases with the increase in doping whatever the value of absorber thickness; this can be due to the most recombination process. This result is in agreement with Ouédraogo *et al.* [13]. The increase of FF with the acceptor density in the range of 2×10^{16} to 4×10^{16} cm^{-3} is due to weak recombination phenomenon in the depletion region. On the other hand, the decrease of FF for acceptor density greater than 4×10^{16} cm^{-3} produces an increase in the bulk recombination [17]. When the absorber thickness decreases, a small quantity of photons is absorbed and the quantity of pair electron-hole decreases; this leads to the decrease of the solar cell efficiency [13]. The low increase of the efficiency with the absorber thickness [Fig. 7(d)] is related to the combined effects of the low decrease of J_{SC} and the strong increase of V_{OC}.

3.6. *Effect of the P+ layer on the electrical parameters*

According to Igalson *et al.*, the J–V curves and photovoltaic parameters of the CIGS cells depend on the window and interface properties of the cell [25]. The P+ layer increases the recombination mechanism at the CdS/CIGS interface and, thus reduces the electrical parameters of the cell [24]. In this part, the acceptor densities in the absorber layer and those of the donor in the CdS layer have been fixed respectively at 5×10^{16} and 8×10^{18} cm^{-3}. Then, we studied the acceptor concentration in the P+ layer and its thickness on the J–V parameters. Figure 8 shows the influence of acceptors density of the P+ layer on the electrical parameters. J_{SC}, FF and the efficiency decrease and follow the same trend when the thickness and the acceptors concentration of P+ layer increase. These results are in agreement with the results of Ref. 26, which showed that the fill factor losses depend on the width and concentration of acceptor in the P+ layer representing V_{se}-V_{cu} defects in the acceptors' configuration. It has been shown that the high negative charge density in the P+ layer leads to a reduced voltage drop within the absorber layer. The built-in electric field in the space charge region of the CIGS layer is therefore lowered, resulting in a worse FF [27]. However, the reduction of the acceptors density in the P+ layer from 8×10^{16} to 2×10^{16} cm^{-3} [Fig. 8(d)], with the thickness of 10 nm, leads to an optimal efficiency close to 18.50%. In addition, the degradation of the efficiency with increase of the

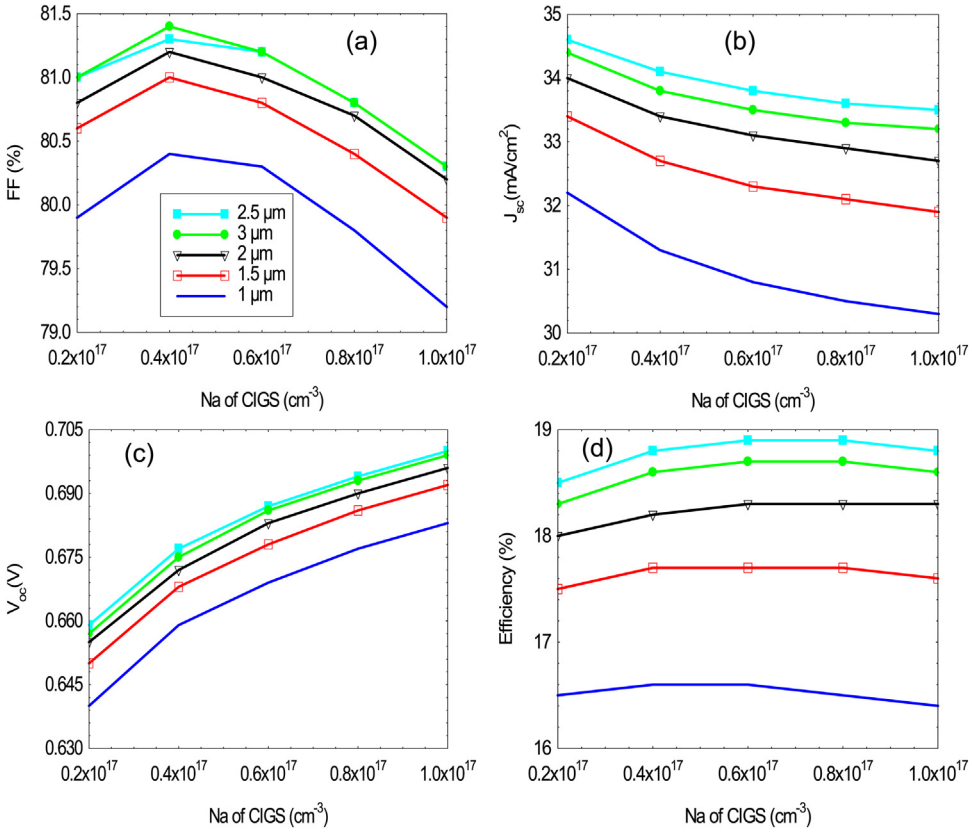

Fig. 7. Evolution of the electrical parameters (V_{OC}, J_{SC}, FF and η) as a function of the absorber layer thickness and acceptor density.

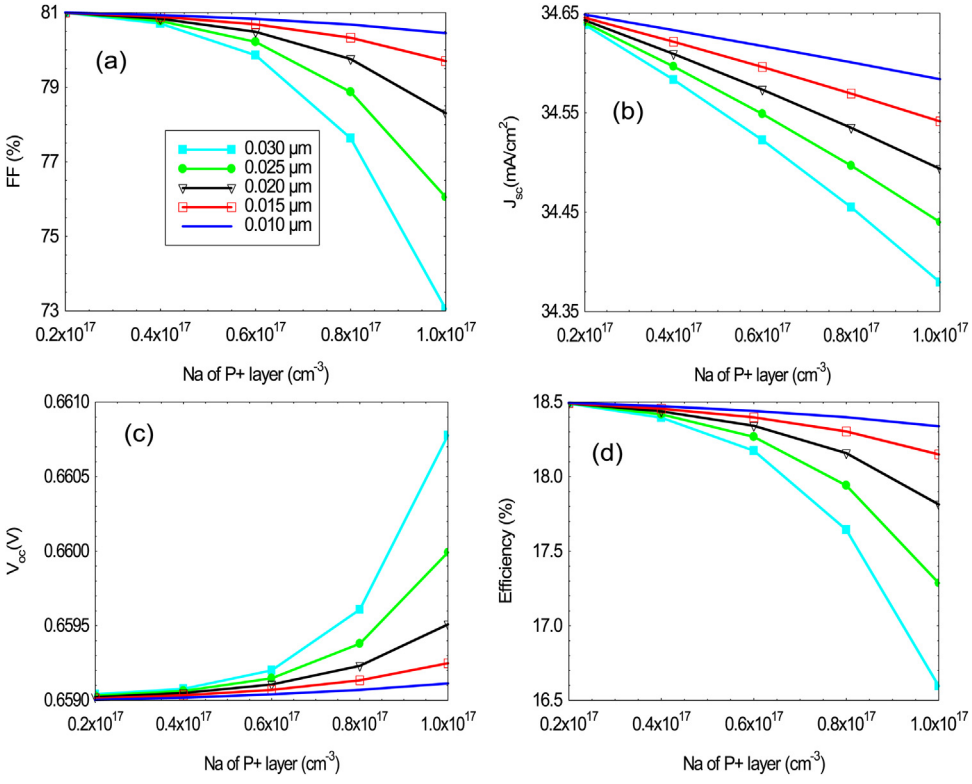

Fig. 8. Influence of the P+ layer acceptors' density on electrical parameters of the cell according to thickness: (a) FF, (b) J_{SC} (c) V_{OC} and (d) efficiency.

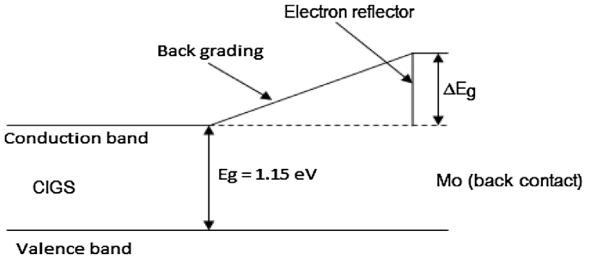

Fig. 9. Different scenarios of BSF at the back contact. (i) adapt the work function of the back metal in order to obtain the desired band bending on the CIGS layer, (ii) insert a highly doped p-type layer at the CIGS/Mo interface, (iii) linear increase in Ga content at the back (Back-grading).

Table 3
Parameters of various layers BSF [21].

Parameters	BSF
W [μm]	0.01
E_g [eV]	variable
$\varepsilon/\varepsilon_0$	13.6
N_C [cm^{-3}]	2.2×10^{18}
Nv [cm^{-3}]	1.8×10^{19}
v_h^e [cm/s]	10^7
v_{th}^p [cm/s]	10^7
μ_e [cm^2/Vs]	100
μ_p [cm^2/Vs]	25
Doping [cm^{-3}]	variable

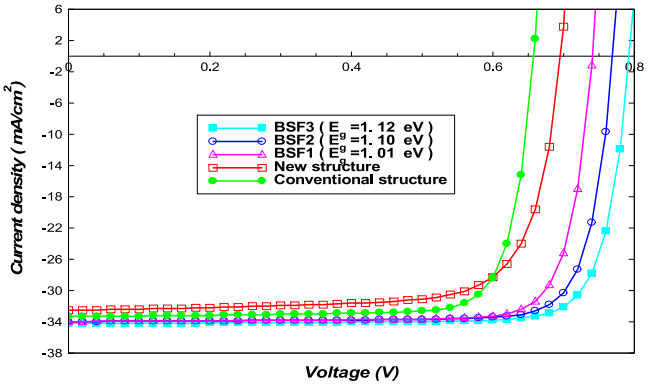

Fig. 10. Current – voltage characteristics of conventional structure and the new structure with BSF at the CIGS/Mo interface.

Table 4
Comparison of the electrical parameters of various structures.

Structure of the solar cell	V_{OC} (V)	J_{SC} (mA/cm^2)	FF (%)	η (%)
i-ZnO/CdS/OVC/CIGS/Mo	0.6959	32.529	75.26	17.70
i-ZnO/CdS/P+/CIGS/Mo	0.6579	33.342	80.99	18.46
i-ZnO/CdS/P+/CIGS/BSF(E_g = 1.01 eV)/Mo	0.74	34.84	81.92	21.59
i-ZnO/CdS/P+/CIGS/BSF(E_g = 1.10 eV)/Mo	0.76	34.85	82.04	22.51
i-ZnO/CdS/P+/CIGS/BSF(E_g = 1.12 eV)/Mo	0.79	34.86	82.59	23.34

thickness and the doping concentration of the P+ layer is related to the reduction of FF and J_{SC}.

A thick layer and a higher doping of the P+ layer degrade the performances of solar cell. An efficiency of 18.50% is obtained for a thickness of 10 nm and a concentration N_a of 2×10^{16} cm^{-3} in the P+ layer. In the following sections, these parameters will be used to optimize the new structure (Fig. 9).

3.7. Solar cell for high performance

To optimize the new structure, we have inserted a high band-gap layer commonly called Back Surface Field (BSF) at the CIGS/Mo interface. This becomes very important for electrons generated close to the black contact, which have high probability for back contact recombination when the thickness of the absorber is reduced [28]. The BSF creates a potential barrier for the electrons while having an ohmic behaviour with the holes. Experimentally, three approaches are generally used to create this barrier: (i) adapt the work function of the back metal in order to obtain the desired band bending on the CIGS layer, (ii) insert a highly doped p-type layer at the CIGS/Mo interface along with a relatively wide gap for a good transparency. This is generally achieved by inserting a very thin layer of $CuGaSe_2$ at the CIGS/Mo interface [29], (iii) a linear increase in Ga content at the back (Back-grading) [15]. These three situations have been represented in Fig. 8. A comparative study of these different approaches has been done by Gloeckler *et al.* [15]. In our case, we used the approach (ii). We fixed the thickness of the buffer layer, as well as the donor density at 50 nm and 8×10^{18} cm^{-3}, respectively. The absorber acceptor density is also set at 5×10^{16} cm^{-3}. However, to appreciate the influence of the BSF layer, we reduced the absorber thickness to 1 μm. The parameters of the other layers are identical to those of Table 1. The doping of the BSF is chosen so that it should be greater than that of the absorber. The other parameters of the BSF layer are shown in Table 3.

Figure 10 shows the behaviour of the J–V characteristics as function of the BSF layer bandgap, and compared with the two previous structures (Fig. 1). It is noticed that, the more the bandgap of the BSF increases, the better is the efficiency of the cell. This is explained by the fact that increase of the BSF layer bandgap also increases the potential barrier in the rear contact. This effect reduces the recombination of minority carriers at the back contact of the cell, by having an ohmic behaviours of the majority carriers (holes). Efficiency of 21.59%, 22.51% and 23.34% (Table 4), corresponding respectively to 1.01 eV, 1.10 eV and 1.12 eV BSF layer bandgap, are obtained within this simulation. The role of the BSF layer is in agreement with the results carried out by Teyou *et al.* [30] in the case of CdTe-based solar cell. Add the BSF layer at the CIGS/Mo improves V_{OC} and seems to have a low influence on J_{SC} and FF parameters (Table 4). According to Gloeckler *et al.* when the thickness of the absorber is between 0.4 and 1 μm, a larger back barrier gives rise to a larger back-contact depletion region, which attracts light-generated carriers and increases J_{sc} losses [15], which is in good agreement with our results. The increase of the gap band of BSF as a function of the variation of its doping increases the electrical parameters of the cell. An efficiency of 21.59%, 22.51% and 23.34%, respectively correspond to a BSF band-gap of 1.01 eV, 1.10 eV and 1.12 eV for a variation of its respective doping of 4×10^{16}, 6×10^{16} and 8×10^{16} cm^{-3} are obtained in this simulation. Generally, the BSF layer provides an average gain of 3 mA/cm^2 of the current density. This is in agreement with the references' results [4,11,30].

We have summarized in Table 4 the electrical parameters of various configurations of CIGS-based solar cells.

Based on the results presented in Table 4, structures containing BSF layer, present better efficiency compared to those of conventional and new structure without BSF layer. The presence of BSF layer in the solar cell structure has as a role to avoid the recombination phenomenon at the Mo/CIGS interface, by reflecting the minority carriers towards the main junction. The presence of BSF layers in the cell structure improves the electrical parameters of the solar cell (Table 4).

3.8. Effect of the temperature

Operating temperature plays an important role in the performance of CIGS solar cell. Figure 11 shows the effect of temperature on the conversion efficiency of various structures of solar cells.

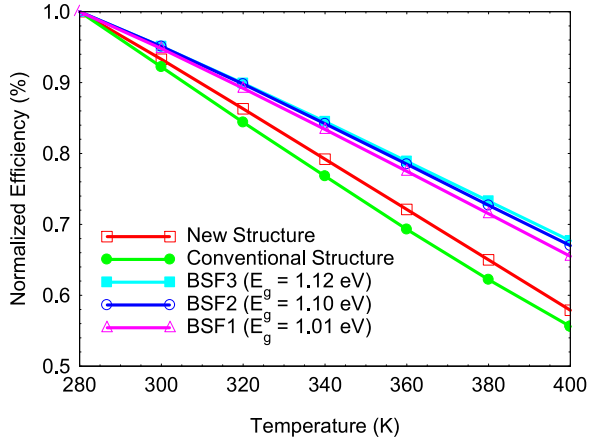

Fig. 11. Effect of the operating temperature on the normalized efficiency.

As can be seen, the conversion efficiency decreases linearly with the increase of the operating temperature. The declination of the efficiency with the temperature are -0.37%/K and -0.35%/K for the conventional structure and the new structure, respectively. Many studies have shown that temperature affects the optical, structural and electrical properties of CIGS based solar cells. The recombination mechanisms become more important when the temperature increases due to the modification of the band-structures. The difference of temperature coefficients between the conventional structure and the new structure is due to the presence of SDL or P+ layer at the CdS/CIGS interface. The CIGS solar cell containing the SDL layer at the CdS/CIGS interface has a better stability than the one containing the P+ interface layer. Because the SDL layer reduces, recombination at the interface of the junction thus allows the CIGS cell to have a good coefficient compared to the P+ layer, which instead increases the recombinations at the interface CdS/CIGS by lowering the Fermi level of the interface.

When the BSF layer is introduced into the back contact of the new structure, there is an improvement in the stability.

4. Conclusions

In this study, the role of junction configuration and its impact are numerically investigated, using SCAPS-1D software. We varied absorber, buffer and P+ layers thickness, as well as donors and acceptors density in order to get optimal performances. We showed that increasing acceptors density in the absorber layer leads to a reduction of solar cell performances. For instance, short-circuit current is reduced of about 3.8 mA/cm^2 due to increasing recombination in the bulk of the absorber. The P+ layer, present at the interface of the absorber and the buffer layer in the structure of a CIGS-based solar cell, is less beneficial than the OVC layer. We noticed that whatever the absorber thickness, good performances are obtained when acceptors density is between 2×10^{16} cm^{-3} - 8×10^{16} cm^{-3}. The efficiency and the fill factor of our numerical sample is of 18.85% and 81.9%, respectively. Our results obtained from these simulations are in good agreements with experimental results. Our study also shows that a thicker CdS buffer layer reduces cell's efficiencies; therefore, it seems important to reduce it. Increasing doping concentration in buffer and P+ layers decreases cell's parameters. However, different BSF layers were introduced between the CIGS layer and back contact in order to get high efficiencies with a thinner absorber layer. BSF layer with a large bandgap (most reflecting minority carrier) leads to better efficiency. When using this configuration, better thermal stability and efficiency of -0.27%K and 23.34% are obtained, respectively.

Conflict of interests

The authors declare that there is no conflit of interests regarding the publication of this paper.

CRediT authorship contribution statement

N. Guirdjebaye: Conceptualization, Methodology, Software, Writing - original draft.

S. Ouédraogo: Conceptualization, Methodology, Software, Writing - original draft, Validation, Project administration.

A. Teyou Ngoupo: Conceptualization, Methodology, Software, Writing - original draft.

G.L. Mbopda Tcheum: Data curation, Methodology, Software, Writing - original draft.

J.M.B. Ndjaka: Conceptualization, Methodology, Supervision, Validation.

Acknowledgements

The authors acknowledge the use of SCAPS-1D program developed by Marc Burgelman and colleagues at the University of Gent in all the simulations reported in this work

References

[1] P. Jackson, D. Hariskos, E. Lotter, S. Paetel, R. Wuerz, R. Menner, W. Wischmann, M. Powalla, Prog. Photovolt: Res. Appl. 19 (2011) 894.
[2] P. Jackson, *et al.*, Effects of heavy alkali elements in Cu(In,Ga)Se_2 solar cells with efficiencies up to 22.6%, Physica Status Solidi (RRL) Rapid Res. Lett. 10 (8) (2016) 583–586.
[3] V.S. Saji, I.H. Choi, C.W. Lee, Progress in electrodeposited absorber layer for $CuIn_{(1-x)}GaxSe_2$ (CIGS) solar cells, Sol. Energy 85 (11) (2011) 2666–2678.
[4] O. Lundberg, M. Edoff, L. Stolt, The effect of Ga-Grading in CIGS thin film solar cells, Thin Solid Films 480-481 (2005) 520–525.
[5] M.J. Romero, K.M. Jones, J. AbuShama, Y. Yan, M.M. Al-Jassim, R. Noufi, Surface-layer band gap widening in Cu(In, Ga)Se_2 thin films, Appl. Phys. Lett. 83 (23) (2003) 4731–4733.
[6] Y. Yan, K.M. Jones, J. Abushama, M. Young, S. Asher, M.M. Al-Jassim, R. Noufi, Microstructure of surface layers in Cu(In,Ga)Se_2 thin films, Appl. Phys. Lett. 81 (6) (2002) 1008–1010.
[7] Z. Li, X. Yu-Ming, X. Chuan-Ming, H. Qing, L.F. Fang, L. Chang-Jian, S. Yun, Microstructural characteriszation of Cu-poor Cu(In,Ga)Se_2 surface layer, Thin Solid Films 520 (2012) 2873–2877.
[8] D. Liao, A. Rockett, Cd doping at the $CuInSe_2$/CdS heterojunction, J. Appl. Phys. 93 (11) (2003) 9380–9382.
[9] Y. Okano, T. Nakada, A. Kunioka, XPS analysis of CdS/$CuInSe_2$ heterojunction, Sol. Energy Mater. Sol. Cells 50 (1998) 105.
[10] M.J. Romero, K.M. Jones, J. AbuShama, Y. Yan, M.M. Al-Jassim, R. Noufi, Surface- layer band widening in Cu(In,Ga)Se_2 thin films, Appl. Phys. Lett. 83 (2003) 4731.
[11] Chia-Hua Huang, Effects of junction parameters on Cu(In;Ga)Se2 solar cells, J. Phys. Chem. Solids 69 (2008) 779, 69, 779.
[12] A. Niemegeers, M. Burgelman, R. Herberholz, U. Rau, D. Hariskos, H.-W. Schock, Model for electronic transport in Cu(In,Ga)Se_2 solar cells, Prog. Photovolt. Res. Appl. 6 (1998) 407–421.
[13] S. Ouédraogo, F. Zougmoré, J.M.B. Ndjaka, Computational analysis of the effect of the surface defect layer (SDL) properties on Cu(In,Ga)Se_2-based solar cell performances, J. Phys. Chem. Solids 75 (5) (2014) 688–695.
[14] S. Ouedraogo, R. Sam, F. Ouedraogo, M.B. Kebre, F. Zougmore, J.M. Ndjaka, Optimization of copper indium gallium Di-selenide (CIGS) based solar cells by back grading, in: AFRICON IEEE, 2013, 1–6.
[15] M. Gloeckler, J.R. Sites, Potential of submicrometer thickness Cu(In, Ga)Se_2 solar cells, J. Appl. Phys. 98 (10) (2005) 103703.
[16] Y. Hagiwara, T. Nakada, A. Kunioka, Improved Jsc in CIGS thin film solar cells using a transparent conducting ZnO:B window layer, Sol. Energy Mater. Sol. Cells 67 (2001) 267–271.
[17] M.A. Contreras, L.M. Mansfield, B. Egaas, J. Li, M. Romero, R. Noufi, W. Mannstadt, Improved energy conversion efficiency in wide band-gap Cu(In, Ga)Se_2 solar cells, 2011, Photovoltaic Specialists Conference (*PVSC*), 37th IEEE (2011) 000026–000031.
[18] S. Degrave, M. Burgelman, P. Nollet, Modelling of polycrystalline thin film solar cells: new features in SCAPS version 2.3, 2003, Photovoltaic Energy Conversion 1 (2003) 487–490.
[19] A. Hultqvist, C. Platzer-Björkman, E. Coronel, M. Edoff, Experimental investigation of Cu(In_{1-x},Ga_x)Se2/Zn (O_{1-z}, S_z) solar cell performance, Sol. Energy Mater. Sol. Cells 95 (2) (2011) 497–503.

[20] S. Ouédraogo, F. Zougmoré, J.M. Ndjaka, Numerical analysis of copper-indium-gallium-diselenide-based solar cells by SCAPS-1D, Int. J. Photoenergy (2013), http://dx.doi.org/10.1155/2013/421076.
[21] M. Topic, F. Smole, J. Furlan, Examination of blocking current-voltage behaviour through defect chalcopyrite layer in ZnO/CdS/Cu(In,Ga)Se_2/Mo solar cell, Sol. Energy Mater. Sol. Cells 49 (1997) 311–317.
[22] D. Hariskos, S. Spiering, M. Powalla, Buffer layers in Cu(In, Ga)Se_2 solar cells and modules, Thin Solid Films 480 (2005) 99–109.
[23] S.H. Demtsu, J.R. Sites, Quantification of losses in thin-film CdS/CdTe solar cells, Photovoltaic Specialists Conference (2005) 347–350..
[24] M. Igalson, P. Zabierowski, D. Przado, A. Urbaniak, M. Edoff, W.N. Shafarman, Understanding defect-related issues limiting efficiency of CIGS solar cells, Solar Energy Mater. Solar Cells 93 (2009) 1290–1295.
[25] M. Igalson, P. Zabierowski, Electron traps in Cu(In,Ga)Se_2 absorbers of thin solar cells studied by junction capacitance techniques, Opto-electron. Rev. 11 (4) (2003) 261–267.
[26] M. Igalson, M. Bodegard, L. Stolt, Reversible changes of the fill factor in the ZnO/CdS/Cu(In,Ga)Se_2 solar cells, Sol. Energy Mater. Sol. Cells 80 (2003) 195–207.
[27] M. Topic, F. Smole, J. Furlan, Examination of blocking current-voltage behaviour through defect chalcopyrite layer in ZnO/CdS/Cu(In,Ga)Se_2/Mo solar cell, Sol. Energy Mater. Sol. Cells 49 (1997) 311–317.
[28] S. Ouedraogo, R. Sam, F. Ouedraogo, M.B. Kebre, F. Zougmore, J. Ndjaka, M:Modélisation numérique d'une cellule solaire à couches minces à base de CIGS, thèse de doctorat Ph/D, à l'Université de de Ouagadougou, Burkina Faso, 2015 (IN FRENCH).
[29] O. Lundberg, M. Bodegard, J. Malmstrom, L. Stolt, Influence of the Cu(In,Ga)Se_2 thickness and Ga grading on solar cell performance, Prog. Photovolt: Res. Appl. 11 (2003) 77–88.
[30] A. Teyou Ngoupo, S. Ouédraogo, F. Zougmoré, J.M.B. Ndjaka, New architecture towards ultrathin CdTe solar cells for high conversion efficiency, Int. J. Photoenergy (2015), http://dx.doi.org/10.1155/2015/961812.